Photothermally Enhanced Photodynamic Therapy Delivered by Nano-Graphene Oxide

Bo Tian, Chao Wang, Shuai Zhang, Liangzhu Feng, and Zhuang Liu*

Jiangsu Key Laboratory for Carbon-Based Functional Materials & Devices, Institute of Functional Nano & Soft Materials (FUNSOM), Soochow University, Suzhou, Jiangsu, 215123, People's Republic of China

ABSTRACT Graphene with unique physical and chemical properties has shown various potential applications in biomedicine. In this work, a photosensitizer molecule, Chlorin e6 (Ce6), is loaded on polyethylene glycol (PEG)-functionalized graphene oxide (GO) *via* supramolecular $\pi-\pi$ stacking. The obtained GO-PEG-Ce6 complex shows excellent water solubility and is able to generate cytotoxic singlet oxygen under light excitation for photodynamic therapy (PDT). Owing to the significantly enhanced intracellular trafficking of photosensitizers, our GO-PEG-Ce6 complex offers a remarkably improved cancer cell photodynamic destruction effect compared to free Ce6. More importantly, we show that the photothermal effect of graphene can be utilized to promote the delivery of Ce6 molecules by mild local heating when exposed to a near-infrared laser at a low power density, further enhancing the PDT efficacy against cancer cells. Our work highlights the promise of using graphene for potential multifunctional cancer therapies.

KEYWORDS: graphene · Chlorin e6 · photodynamic therapy · photothermal effect · combined therapies

sp^2 carbon nanomaterials especially carbon nanotubes have attracted significant interest in the area of nanomedicine in the past decade. Functionalized carbon nanotubes have been widely explored as drug delivery vehicles for potential cancer treatment, contrast agents in different imaging modalilties, and novel biosensor nanoplatfroms.[1−5] Graphene, a single or few-layered two-dimensional (2D) sp^2-bonded carbon sheet, is another class of sp^2 nanocarbons and exhibits many outstanding properties in physics and chemistry. Since its discovery in 2004, graphene has been extensively studied in many different fields including nanoeletronics, composite materials, energy research, catalysis, and more recently biomedicine.[6−20] Utilizing the interesting optical, electrical, and chemical properties of graphene, various graphene-based biosensors have been fabricated to detect biomolecules with high sensitivities.[12,21−30] Graphene has a polyaromatic surface structure with an ultrahigh surface area, which is available for efficient loading of aromatic drug molecules *via* $\pi-\pi$ stacking for applications in drug delivery.[13,14,31−34] Recently, we and others have also demonstrated effective gene delivery with graphene nanovectors.[35,36] Owing to its high optical absorption in the near-infrared (NIR) region, PEGylated graphene oxide (GO-PEG) has also been used for efficient photothermal ablation of tumors in animal experiments in our recent study.[16] Our latest work[37] used a radiolabeling method to study the pharmacokinetics and biodistribution of intravenously injected GO-PEG in mice, observing gradual renal and fecal clearance, which was confirmed by direct counting of GO-PEG aggregates in the mouse liver. Systematic serum chemistry, complete blood panels, and histological assays all showed that GO-PEG at our injected dose (20 mg/kg) was not obviously toxic at least to mice. Those results encourage the future exploration of graphene-based nanomedicine for novel cancer therapies.

Photodynamic therapy (PDT) is known as a noninvasive medical technology to treat diseases such as cancer. In the process of PDT, the photosensitizer (PS) molecule transfers the photon energy to surrounding oxygen molecules to generate reactive oxygen species (ROS) such as singlet oxygen to kill cancer cells under the irradiation of light with appropriate wavelengths.[38−40] Compared to traditional chemotherapies and radiotherapies, PDT cancer treatment shows remarkably reduced side effects and improved selectivity since only the lesion that is exposed to the light is treated, while other tissues in the dark are not affected. To increase the water solubility of PS molecules and improve their delivery into cancer cells, various nanocarriers have been actively developed for the delivery of PDT agents.[41]

Clinical hyperthermia methods, including incubation chambers, limb perfusion, and

* Address correspondence to zliu@suda.edu.cn.

Received for review April 28, 2011 and accepted August 4, 2011.

Published online August 04, 2011
10.1021/nn201560b

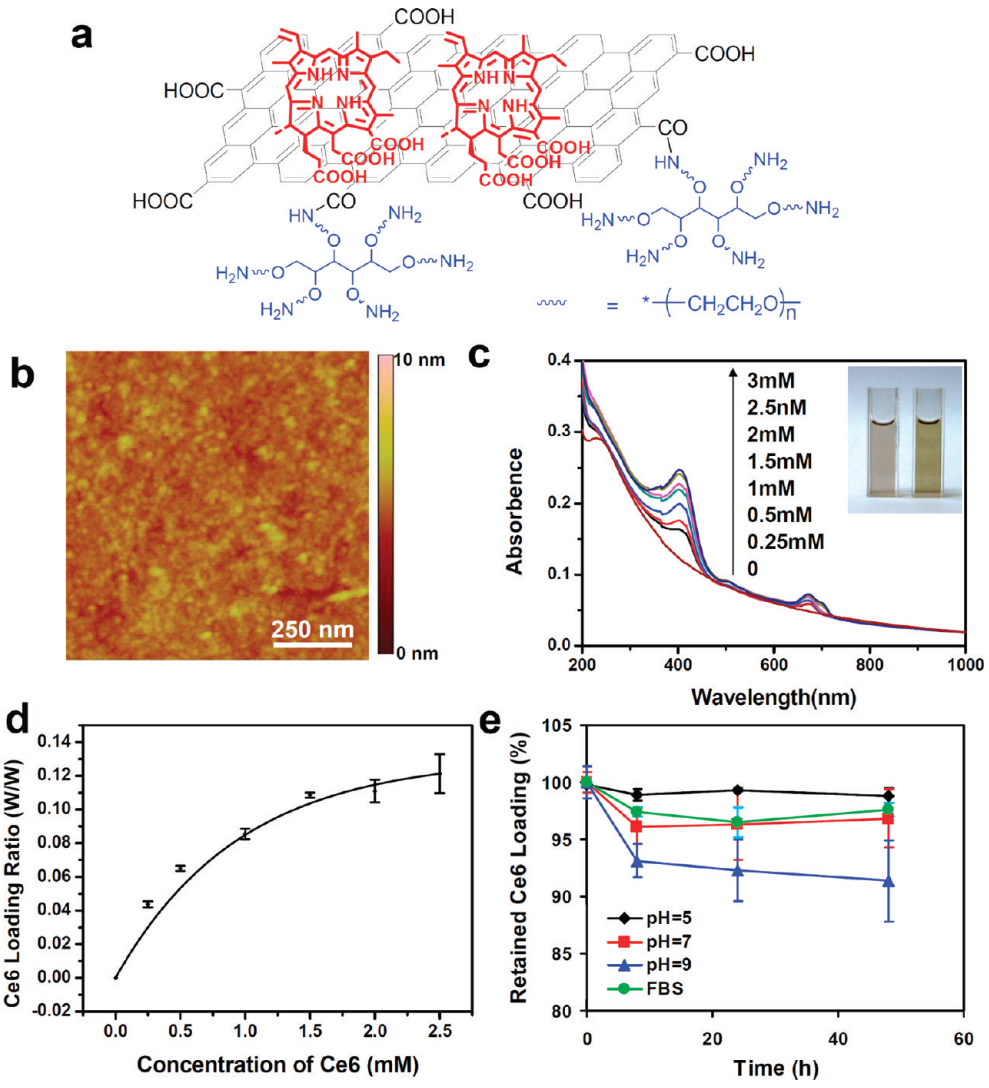

Figure 1. Loading of Ce6 on GO-PEG. (a) Schematic drawing showing Ce6 loading on GO-PEG. Red: Ce6; black: GO; blue: six-arm PEG. (b) AFM image of GO-PEG. (c) UV−vis spectra of GO-PEG-Ce6 at different Ce6 feeding concentrations. Inset: photo of GO-PEG (left) and GO-PEG-Ce6 (right) solutions. (d) Relationship between the feeding Ce6 concentrations and the amounts of Ce6 loaded on GO-PEG. (e) Release of Ce6 from GO-PEG-Ce6 in PBS. Error bars were based on standard deviations (SD) of triplicate samples.

radiowave irradiation, are able to increase the lesion temperature, improving the therapeutic effect of chemotherapy drugs.[42−45] However, such nonspecific heating may also increase the toxicity of chemotherapy to normal organs. In recent years, photothermal therapy using optical absorbing nanomaterials including graphene has been widely applied to "cook" cancer cells at high temperatures above 50 °C under NIR light irradiation.[16,46−51] On the other hand, it has been demonstrated in a recent work that mild photothermal heating to ~43 °C by lower power NIR laser irradiation of FeCo/graphitic nanoparticles was able to enhance the intracellular delivery of a chemotherapy drug, doxorubicin, for improved cancer cell killing.[52]

In this work, we show that nanographene can be an excellent nanoplatform for PDT delivery, whose efficiency is further improved by the unique photothermal treatment. Branched PEG-functionalized nanographene oxide (GO-PEG) is loaded with Chlorin e6 (Ce6) *via* $\pi-\pi$ stacking. The graphene-based PDT delivery offers dramatically increased intracellular shuttling of Ce6, largely enhancing the light-induced cancer cell killing efficiency. Interestingly, we uncover that graphene with high NIR absorption is able to produce local heating under NIR laser irradiation at mild conditions, increasing the cellular uptake of GO-PEG-Ce6 by approximately 2-fold and thus further enhancing the cancer cell killing during PDT treatment. Our data show the promise of using graphene in combined phototherapies of cancer with synergistic efficacies.

RESULTS AND DISCUSSIONS

Graphene oxide (GO) was conjugated to amine-terminated six-armed PEG *via* amide formation following our previously reported procedures and then loaded with Ce6 *via* supramolecular $\pi-\pi$ stacking

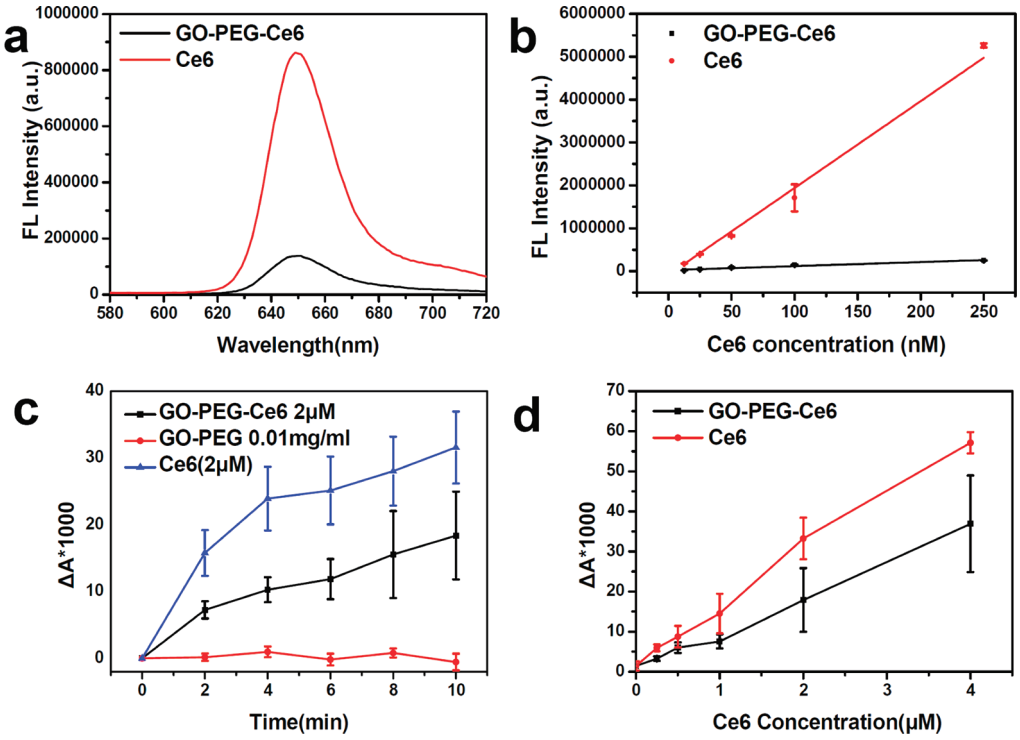

Figure 2. Fluorescence and singlet oxygen generation data of GO-PEG-Ce6 and free Ce6. (a) Fluorescence spectra of GO-PEG-Ce6 and free Ce6 at 100 nM of Ce6 equivalent under 400 nm excitation. (b) Fluorescence intensities of GO-PEG-Ce6 and free Ce6 at different concentrations. (c) Time-course generation of singlet oxygen by GO-PEG-Ce6 and free Ce6 at 2 μM of Ce6 equivalent under 660 nm laser irradiation (0.1 W/cm^2). (d) Generation of singlet oxygen by GO-PEG-Ce6 and free Ce6 at different concentrations after 660 nm laser irradiation (0.1 W/cm^2) for 10 min. The decreased RNO absorbance at 440 nm (ΔA) was in linear relationship to the concentration of generated singlet oxygen. Error bars were based on the SD of triplicated samples.

(Figure 1a), which was a strategy widely used to load aromatic chemotherapy drugs (*e.g.*, doxorubicin) on the surface of sp^2-bonded nanocarbons such as graphene and carbon nanotubes.[13,14,31,53,54] PEGylated nanographene (GO-PEG) exhibited excellent stability in a range of physiological solutions including saline, cell medium, and serum (Supporting Figure S1).[13,14,16] Atomic force microscope (AFM) imaging showed that the size of GO-PEG was less than 50 nm and the thickness was about 1 nm (Figure 1b). After mixing GO-PEG with varied concentrations of Ce6 in phosphate-buffered saline (PBS) overnight and the followed purification to remove free Ce6, successful Ce6 loading on GO-PEG was evidenced by UV−vis spectra of GO-PEG-Ce6, in which the characteristic Ce6 absorption peaks were clearly identified (Figure 1c). The UV−vis peak at 404 nm was then used to determine the concentrations of Ce6 in GO-PEG-Ce6 samples after subtraction of absorbance contributed by GO-PEG. We investigated the relationship between the feeding concentrations of Ce6 and the amount Ce6 finally loaded on GO-PEG by UV−vis spectra (Figure 1c and d). It was found that the loading capacity (the weight ratio of Ce6:GO in the GO-PEG-Ce6 sample) of Ce6 on GO-PEG reached a maximum of 15% at Ce6 concentrations above 3 mM. We chose 1 mM Ce6 as the appropriate feeding concentration ($m_{Ce6}/m_{GO\text{-}PEG} \approx 0.11$) in our following experiments. Although the loading of Ce6 on GO-PEG is less efficient, excess unloaded Ce6 may be collected and recycled to reduce the cost of future large-scale manufacture. The Ce6 loaded on GO-PEG was rather stable in phosphate buffers with acidic (pH 5) and neutral pH (pH 7), as well as in fetal bovine serum (FBS) (Figure 1e). Due to the deprotonation of carboxyl groups in the Ce6 molecule, its release from GO-PEG was accelerated in basic solutions (*e.g.*, pH = 9). For long-term storage, GO-PEG-Ce6 may be stored in a slightly acidic environment (*e.g.*, pH = 5) to avoid premature release of Ce6.

To understand the interaction between graphene and Ce6, fluorescence spectra of GO-PEG-Ce6 and Ce6 were recorded (Figure 2a). It was uncovered that 80−90% of Ce6 fluorescence was quenched once it was loaded on GO-PEG, likely owing to the direct contact between Ce6 and the graphene sheet (Figure 2a and b). Singlet oxygen generation was the critical step in PDT. We then compared the abilities of singlet oxygen generation between GO-PEG-Ce6 and free Ce6 under irradiation by a 660 nm laser (Figure 2c and d). The generation of singlet oxygen ($^1O_2$) was detected by the bleaching of *N*,*N*-dimethyl-4-nitrosoaniline (RNO), whose absorbance at 440 nm would be diminished in the presence of $^1O_2$.[55] Interestingly, although the fluorescence of Ce6 was drastically

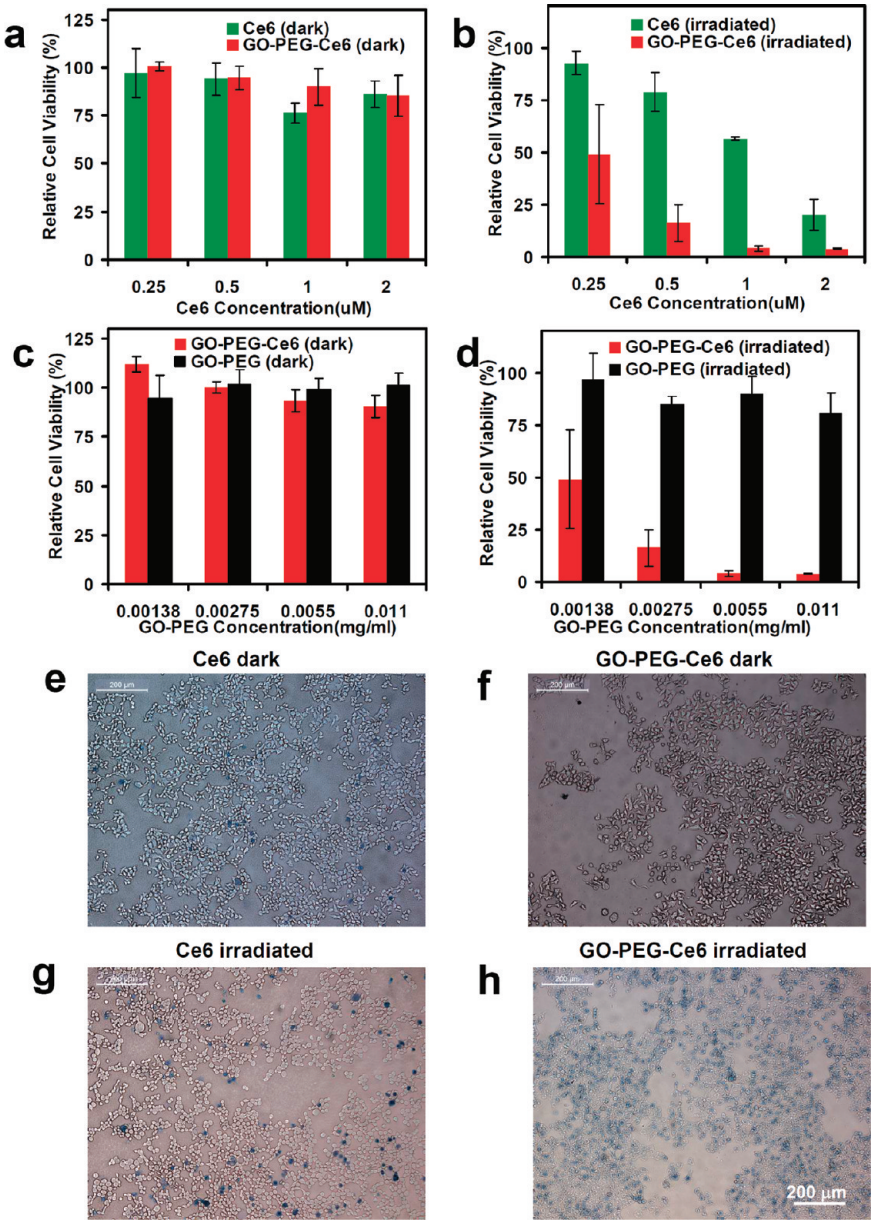

Figure 3. *In vitro* photodynamic cancer cell killing. (a–d) Cell viability data obtained from the MTT assay of KB cells after various treatments indicated. Relative cell viabilities in all samples were normalized to the control saline-added samples without laser irradiation (100% viability). Cells treated with GO-PEG-Ce6 and free Ce6 without (a) and with (b) irradiation by the 660 nm laser (0.1 W/cm^2, 10 min). Cells treated with GO-PEG-Ce6 and GO-PEG without (c) and with (d) light irradiation. The cell viability values were all normalized to control untreated cells. Tyrpan blue stained images of KB cells incubated with Ce6 (e, g) or GO-PEG-Ce6 (f, h) with and without laser irradiation. The Ce6 concentration was 1 μM in e–h. Error bars were based on SD of four parallel samples.

quenched after it was loaded on graphene (10–15% of free Ce6), the $^1O_2$ production ability by GO-PEG-Ce6 was still substantially high (50–60% of free Ce6). We are aware that the quenching effect of $^1O_2$ production from Ce6 by GO-PEG appears to be less drastic compared to that by carbon nanotubes in an earlier study,[56] likely owing to the difference in their structures, as GO has much more surface defects and may be less effective in energy absorbing compared with pristine single-walled carbon nanotubes. The largely retained $^1O_2$ generation efficiency of Ce6 loaded on graphene allows us to use GO-PEG-Ce6 for PDT treatment of cancer cells.

We next tested the graphene-delivered PDT in cellular experiments using human nasopharyngeal epidermal carcinoma KB cells. Cells were incubated with Ce6, GO-PEG, and GO-PEG-Ce6 at a series of concentrations for 24 h and then irradiated with a 660 nm laser at a power density of 0.1 W/cm^2 for 10 min (light dose = 60 J/cm^2). The standard methyl thiazolyl tetrazolium (MTT) assay was carried out to determine relative viabilities of cells at 24 h post various treatments.

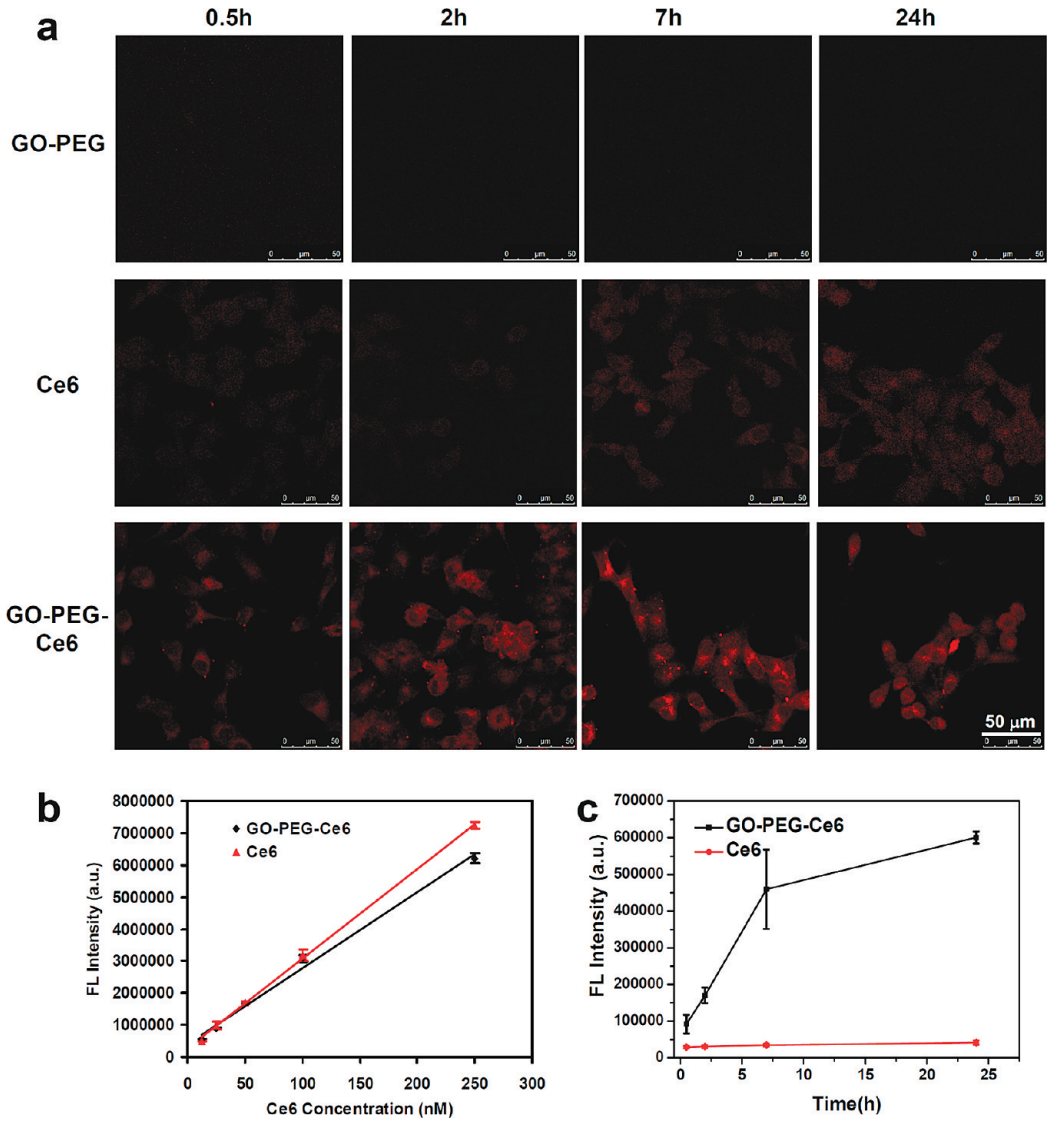

Figure 4. Cellular uptake of Ce6 and GO-PEG-Ce6. (a) Confocal fluorescence images of cells incubated with GO-PEG (upper row), free Ce6 (second row), and GO-PEG-Ce6 (bottom row) after different periods of incubation (0.5, 2, 7, and 24 h). (b) Fluorescence intensities of different concentrations of free Ce6 and GO-PEG-Ce6 solutions after base treatment (12.5, 25, 50, 100, 250 nM). (c) Fluorescence intensities of cell lysate samples from cells incubated with Ce6 and GO-PEG-Ce6 ([Ce6] = 1 μM) for different periods of time (0.5, 2, 7, and 24 h). Error bars were based on SD of triplicate samples.

Without light exposure, GO-PEG-Ce6 and free Ce6 exhibited negligible dark toxicity to KB cells (Figure 3a). Surprisingly, although GO-PEG-Ce6 was less effective in $^1O_2$ generation, its cancer cell killing effect when irradiated by the 660 nm laser was remarkably higher than that of free Ce6 at Ce6 concentrations from 0.25 to 2 μM (Figure 3b). As expected, GO-PEG was not toxic to KB cells either in the dark (Figure 3c) or under light irradiation (Figure.3d). Microscopic images of Trypan blue stained cells further evidenced the improved PDT efficiency of GO-PEG-Ce6 over free Ce6 (Figure 3e–h).

To understand why the PDT effect using GO-PEG-Ce6 was much better than that of free Ce6, we compared their cellular uptake behaviors. KB cells were incubated with GO-PEG-Ce6 or free Ce6 at the same Ce6 concentration (10 μM) for 0.5, 2, 7, and 24 h at 37 °C and then imaged under a confocal fluorescence microscope (Figure 4a). While the intracellular fluorescence increased over time for both Ce6 and GO-PEG-Ce6 incubated cells, the latter showed obviously stronger Ce6 fluorescence inside cells, despite the fluorescence quenching of Ce6 attached on GO-PEG. The localized fluorescence distribution inside cells was possibly owing to the endocytosis[14] of GO-PEG-Ce6 by cells. We then quantitatively measured the cellular uptake of Ce6 and GO-PEG-Ce6 by extracting Ce6 from cell lysate samples. Ce6 molecules loaded on the hydrophobic graphene sheets were completely detached after the strong base (NaOH) treatment as indicated by the ~100% recovery of Ce6 fluorescence (Figure 4b), owing to the deprotonation of three carboxyl acid groups in the Ce6 molecule in base. Cell uptake of GO-PEG-Ce6

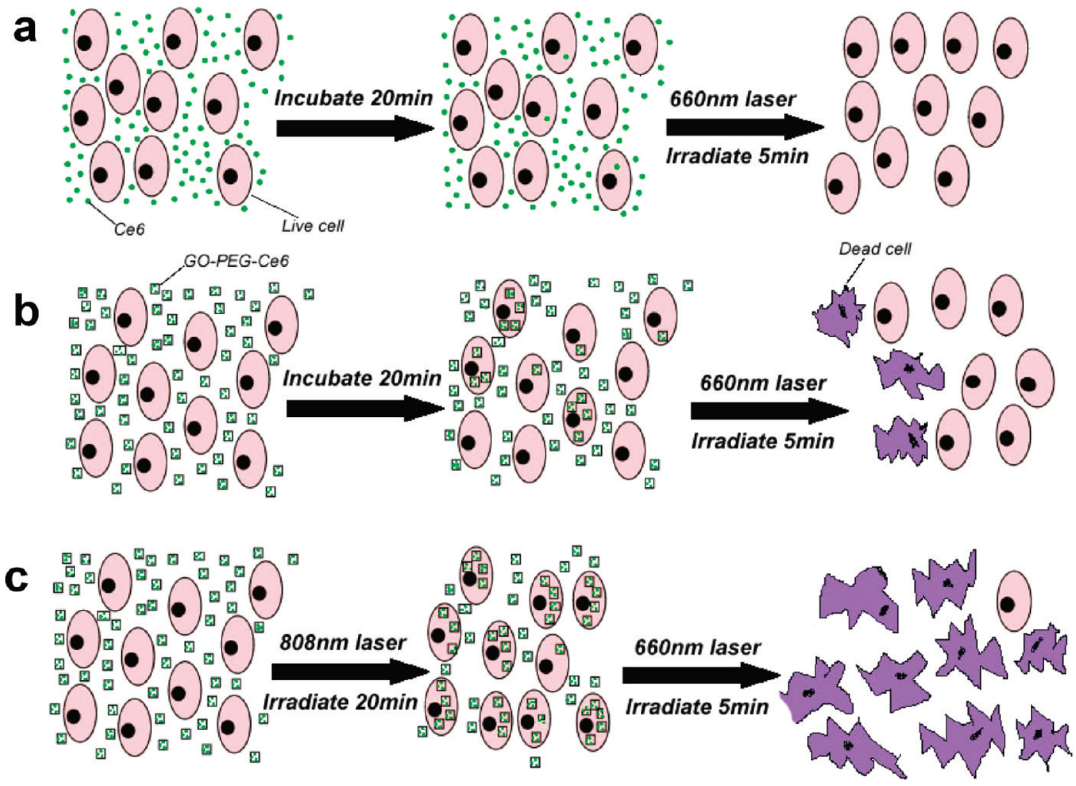

Figure 5. Schemes of the experimental design in photothermally enhanced photodynamic therapy. KB cells were incubated with free Ce6 (a) and GO-PEG-Ce6 (b) for 20 min in the dark and then irradiated by the 660 nm laser (50 mW/cm^2, 5 min, 15 J/cm^2) in control experiments. (c) To induce the photothermal effect, GO-PEG-Ce6 incubated cells were exposed to the 808 nm laser (0.3 W/cm^2, 20 min, 360 J/cm^2) first before PDT treatment.

and Ce6 was quantified by the measured fluorescence intensities of cell lysates after different periods of incubation (0.5, 2, 7, and 24 h) (Figure 4c). The amount of Ce6 delivered into cells by GO-PEG-Ce6 was found to be 1 order of magnitude higher than that of free Ce6, a reason that well explained the remarkably improved efficiency of graphene-delivered PDT (Figure 3). We speculate that the significantly enhanced Ce6 delivery may likely be due to the efficient cell entry of GO-PEG (*e.g.*, by endocytosis[14]) that shuttles Ce6 into cells, while free Ce6 has less effective intracellular cross-membrane diffusion ability.

In our previous work, we have used nanographene for effective photothermal ablation of tumors in a mouse model. Here, we tried to utilize the NIR light absorption ability of GO-PEG to enhance the intracellular delivery of Ce6 for improved PDT efficacy by a mild photothermal treatment. As shown in Figure 5, KB cells were incubated with GO-PEG-Ce6 and irradiated for 20 min by an 808 nm NIR laser at a power density of 0.3 W/cm^2 (360 J/cm^2). Such a laser exposure would induce only mild heating without causing significant cell death. After washing with PBS to remove excess GO-PEG-Ce6, cells were then exposed to the 660 nm laser at a low optical dose of 15 J/cm^2 (50 mW/cm^2, 5 min). Free Ce6 was used as the control (Figure 5a). The nonirradiated samples were incubated in the dark at 37 °C for 20 min before PDT treatment (Figure 5b). It is worth noting that we chose the 808 nm light instead of the 660 nm light by itself for the mild photothermal treatment, not only to differentiate the photothermal and photodynamic effects but also to avoid photobleaching of Ce6 before it is carried into cells.

We first studied the cell uptake of GO-PEG-Ce6 at different conditions by confocal fluorescence imaging. It was found that the cellular uptake of GO-PEG-Ce6 was significant increased after the 808 nm laser irradiation compared to cells incubated in the dark (Figure 6a and b). Increasing the incubation temperature to 43 °C also resulted in the enhanced uptake of GO-PEG-Ce6 by cells (Figure 6c), likely owing to the increased cell membrane permeability at a slightly higher temperature.[52,57] A quantitative cell uptake assay was also conducted to measure the Ce6 fluorescence in cell lysates (Figure 6d and e). At two incubation concentrations (2.5 and 5 μM of Ce6 equivalent), both laser irradiation and direct heating at 43 °C were able to notably increase the cellular uptake of GO-PEG-Ce6 by 2−3-fold.

A cell viability assay was conducted 24 h post PDT treatment at two Ce6 concentrations (2.5 and 5 μM) (Figure 6f and g). Compared to cells incubated with GO-PEG-Ce6 in the dark before 660 nm laser irradiation (50 mW/cm^2, 5 min, equal to 15 J/cm^2), those

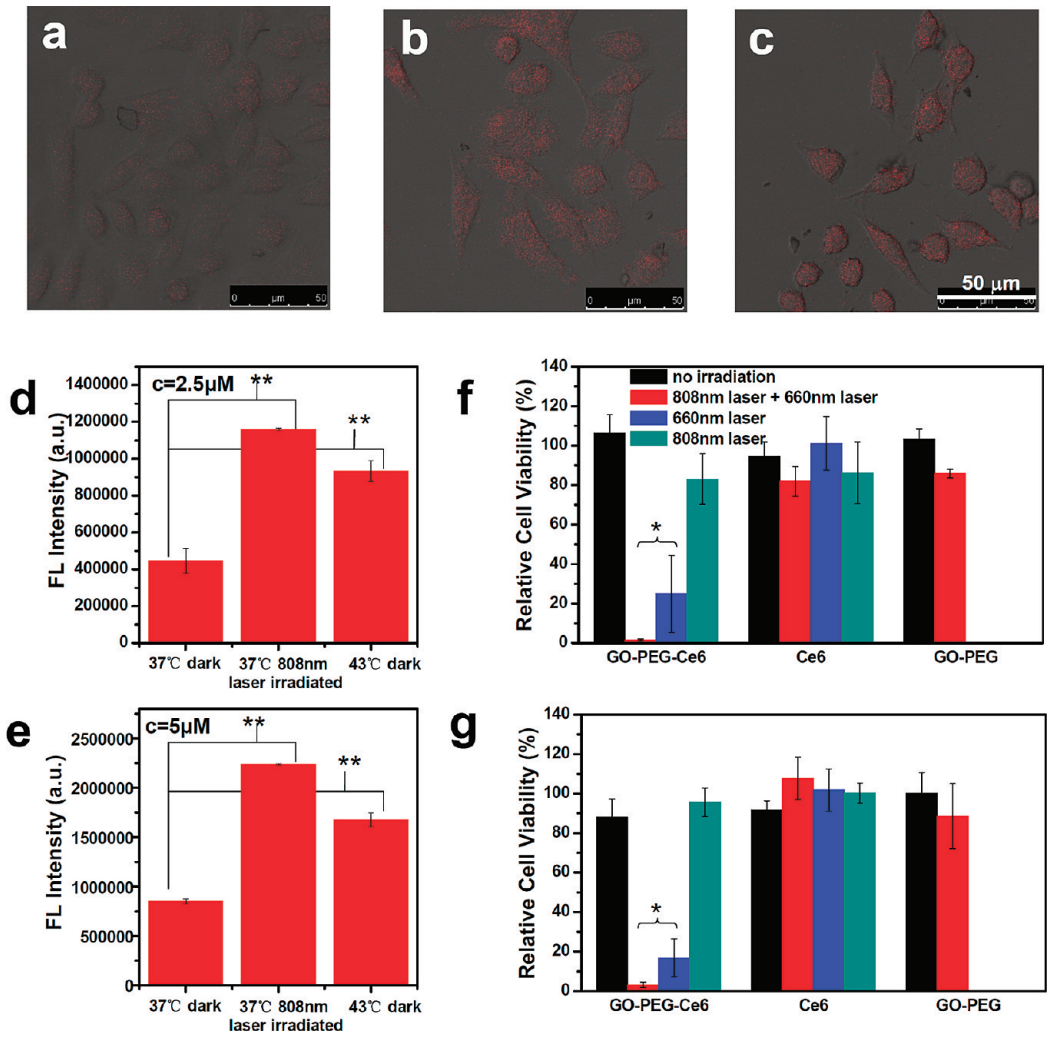

Figure 6. Photothermally enhanced delivery of PDT by graphene. (a–c) Confocal images of KB cells incubated with GO-PEG-Ce6 (5 μM of Ce6 equivalent) at 37 °C with (b) or without (a) 808 nm laser irradiation (360 J/cm^2) and cells incubated at 43 °C in the dark (c). (d, e) Cell uptake of GO-PEG-Ce6 under the three conditions at Ce6 concentrations of 2.5 μM (d) and 5 μM (e) determined by the measured fluorescence intensities of cell lysate samples. (f, g) Cell viability data of KB cells incubated with GO-PEG-Ce6, free Ce6, or GO-PEG respectively at Ce6 concentrations of 2.5 μM (f) and 5 μM (g). Black, red, blue, and green bars represent samples without any light exposure, with both 808 nm (360 J/cm^2) and 660 nm (15 J/cm^2) light irradiation, with only 660 nm light exposure, and with only 808 nm light exposure, respectively. Relative cell viabilities in all samples were normalized to the control saline-added samples without laser irradiation (100% viability). Error bars were based on SD of at least four parallel samples. *P* values were calculated by the student's *t* test: *$p < 0.01$, **$p < 0.001$.

preirradiated by the 808 nm laser (0.3 W/cm^2, 20 min, equals to 360 J/cm^2) and then exposed to the 660 nm laser showed further reduced cell viabilities, owing to the photothermal enhanced cellular uptake of GO-PEG-Ce6. Note that Ce6 has no absorption at 808 nm and cannot be excited by this NIR laser. The power and optical dose of the 660 nm light applied in this experiment were extremely low without causing any noticeable heating of GO-PEG-Ce6 (Supporting Figure S2a). The 808 nm laser irradiation at such a low power was able to generate only mild heating of GO-PEG (temperature increase 5–6 °C, Supporting Figure S2b) and thus by itself induced no obvious cell death to GO-PEG-Ce6-treated cells (Figure 6f and g). The NIR light-induced local heating of nanographene sheets that are close to the cell membrane may contribute to the increased cellular uptake of GO-PEG-Ce6. As the control, no noticeable cell death was observed for Ce6-incubated cells, regardless of laser treatment. An incubation time of 20 min was likely too short to allow sufficient uptake of free Ce6 to offer any appreciable PDT effect. As expected, GO-PEG-incubated cells were essentially not affected after laser irradiations. Our data clearly evidenced that the photothermal effect of graphene was able to enhance the delivery of PDT agents for improved photodynamic cancer cell killing.

Lastly, targeted delivery of photosensitizers to specific types of cancer cells was demonstrated. By conjugating Herceptin (anti-Her2 antibody) to GO-PEG using a well-established protocol,[1,13] actively targeted delivery of PDT to a specific type of Her2 up-regulated cancer cells could also be achieved (Supporting

Figure S3). The antibody-conjugated GO-PEG may potentially be used for targeted photothermal and photodynamic therapy.

CONCLUSION

In this work, we use PEGylated nanographene as a multifunctional nanocarrier to load photosensitizer Ce6 for photothermally enhanced photodynamic therapy. Although GO-PEG-Ce6 shows lower singlet oxygen generation efficiency than free Ce6, the former offers dramatically improved photodynamic cancer cell killing efficacy due to the increased cellular uptake of Ce6 delivered by nanographene. Moreover, we show that the combination of NIR light-triggered mild photothermal heating of graphene and the photodynamic treatment using Ce6 delivered by GO-PEG enhances the PDT efficacy remarkably. The unique physical (strong NIR absorption) and chemical (surface $\pi-\pi$ stacking) properties of PEGylated nanographene oxide are both taken advantage of in this work, showing a synergistic effect in cancer cell destruction. The same strategy may also be applied in graphene-based chemotherapy delivery and gene transfection.[13,14,31,35] Our study demonstrates the controllable multifunctional cancer therapy using graphene and promises future explorations of this class of 2D nanomaterials in nanomedicine.

MATERIALS AND METHODS

Synthesis of GO-PEG. GO-PEG was synthesized following our previous studies.[13,14,37] In brief, graphene oxide was made following a modified Hummers method. NaOH (0.05M) was added to the GO suspension and bath sonicated for about 4 h at 50 °C. The solution was adjusted to pH = 1 using HCl (36% v/v). The resulting solution was neutralized and purified by repeated rinsing and centrifugation. Alkalized graphene oxide (9 mL) at the concentration of ~1 mg/mL was sonicated for 30 min to give a clear solution. A solution of six-armed PEG-amine (Sunbio Inc.) (56 mg/mL, 0.8 mL) was added to the GO solution, and the mixture was sonicated for 5 min. *N*-(3-Dimethylaminopropyl-*N*′-ethylcarbodiimide) hydrochloride (EDC, from Fluka Inc.) was added in two portions to give a final concentration of 5 mM. After overnight reaction, free six-armed PEG-amine was removed by filtration through a 100 kDa filter (Millipore Inc.) and washed with water. The UV/vis absorbency spectrum of the GO-PEG was recorded by a Lambda 750UV/vis/NIR spectrometer (Perkin-Elmer Inc.). The concentration of GO-PEG was determined by the absorbance at 245 nm with a weight extinction coefficient of 65 L g^{-1} cm^{-1}. The formed GO-PEG was stored at 4 °C.

Synthesis of GO-PEG-Ce6. Ce6 (Frontier Scientific Inc.) was dissolved in DMSO at 10 mM as stock solution for further use. GO-PEG (0.2 mg/mL), Ce6 (1 mM), and PBS (0.02 M) were mixed in a 1 mL aqueous solution and incubated overnight. Unadsorbed excess Ce6 was removed by filtration through a 100 kDa filter and washed with water (about six times) until the filtrate became free of green color.

Characterization of GO-PEG-Ce6. The concentration of Ce6 loaded on GO-PEG was determined by the Ce6 characteristic absorption peak at 404 nm with a molar extinction coefficient of 1.1×10^5 M^{-1} cm^{-1} after subtracting the absorbance contributed by GO-PEG at the same wavelength, similar to the measurement of doxorubicin loading on functionalized carbon nanotubes.[53,54] Fluorescence spectra of the GO-PEG-Ce6 and free Ce6 were measured using a Fluoromax-4 spectrofluorometer (Horiba Jobin Yvon Inc.) under 400 nm excitation. To measure the release of Ce6 from GO-PEG-Ce6, a GO-PEG-Ce6 solution was incubated in PBS (pH = 7.4) for different periods of time (0, 3, 7, 12, 24, and 48 h). The amount of retained Ce6 on GO-PEG was measured by UV/vis spectra after removal of detached Ce6 by centrifugal filtration.

Detection of Singlet Oxygen. The generation of singlet oxygen was determined following the Kraljic[55] procedure. Solutions containing GO-PEG-Ce6, GO-PEG, or Ce6 (0, 0.25, 0.5, 1, 2, 4 μM of Ce6; or 0, 0.00125, 0.0025, 0.005, 0.01, 0.02 mg/mL of GO-PEG equivalent, 2 mL of each) were mixed with *p*-nitrosodimethylaniline (25 μM), imidazole (25 μM), and PBS (10 mM, pH = 7.4) and then irradiated by 660 nm laser at the light power density of 0.1 W/cm^2 for different periods of time. The generation of singlet oxygen by Ce6 or GO-PEG-Ce6 would result in the bleaching of RNO absorption at 440 nm. The reduction of optical density at 440 nm thus reflects the production of $^1O_2$.

Photodynamic Treatment and Cell Toxicity Assay. The human nasopharyngeal epidermal carcinoma KB cell line was purchased from American Type Culture Collection (ATCC) and cultured in RPMI-1640 culture medium containing 10% FBS and 1% penicillin/streptomycin at 37 °C under 5% CO_2. For the cell toxicity assay, KB cells were precultured in 96-well cell culture plates at 1×10^4/well for 24 h and then added with GO-PEG-Ce6, free Ce6, or GO-PEG at a series of concentrations. After incubation for 24 h, cells were irradiated by the 660 nm laser at a power density of 0.1 W/cm^2 for 10 min. After another 24 h incubation, the standard MTT (Sigma Inc.) assay was carried out to determine the cell viabilities relative to the control untreated cells (incubated with the same volume of PBS).

Two optical-fiber coupled power-tunable diode lasers (continuous wave) with wavelengths at 660 nm (maximal power = 2 W) and 808 nm (maximal power = 10 W) were both purchased from Hi-Tech Optoelectronics Co. (Beijing, China) and used in this work. The laser beams are round in shape with diameters of 4 and 3 cm, for the 660 and 808 nm laser, respectively, during experiments. The exact optical powers of lasers used in our experiments were calibrated and measured by a LPE-1B laser power/energy meter (Physcience Opto-Electronics Co. Ltd. Beijing).

For photothermally enhanced PDT, KB cells grown in the FBS-containing RMPI-1640 medium were precultured in 96-well cell culture plates at 1×10^4/well for 24 h and then added with GO-PEG-Ce6, free Ce6, or GO-PEG at 2.5 or 5 μM Ce6 equivalent concentrations. The cells were immediately irradiated using the 808 nm laser at a power density of 0.3 W/cm^2 for 20 min (360 J/cm^2). After photothermally heating, cells were irradiated by the 660 nm laser at a power density of 0.05 W/cm^2 for 5 min (15 J/cm^2). After another 24 h incubation, the cell viabilities of samples were determined by the MTT assay.

Cell Uptake Assay. The method of cell uptake assay followed the Ogura procedure.[58] KB cells (1×10^5 cells) grown in the FBS-containing medium were cultured in 35 mm culture dishes containing 1 μM GO-PEG-Ce6 or 1 μM free Ce6 in the dark at 37 °C for different periods of time (0.5, 2, 7, and 24 h). Cells were then washed with PBS three times, harvested using a cell scraper, and then dissolved in 1 mL of 2% sodium dodecyl sulfate for 2 h to obtain homogeneous solutions. One milliliter of 0.2 M NaOH was then added into each culture dish to extract Ce6. Note that Ce6, with three carboxyl acid groups, would be deprotonated and thus detached from GO-PEG in basic solutions. Fluorescence spectra of the obtained solutions were measured under 400 nm excitation.

Trypan Blue Assay. KB cells (2×10^5 cells) grown in the FBS-containing medium cultured in 35 mm culture dishes were added with GO-PEG-Ce6 or free Ce6 at 1 μM of Ce6 equivalent and incubated for 24 h. After irradiation by the 660 nm laser at

the light power density of 0.1 W/cm^2 for 10 min followed by incubation for 24 h, cells was washed with PBS and stained with 0.04% Trypan blue solution (Sigma Inc.) for 5 min. Microscopic images of cells were then taken using a Leica microscope.

Confocal Fluorescence Imaging. KB cells (1×10^5 cells) were cultured with GO-PEG-Ce6 or free Ce6 (Ce6 concentration = 10 μM) in culture dishes. After washing the cells three times with PBS, confocal images of cells were recorded under a Leica SP5 laser scanning confocal microscope (405 nm laser excitation). The emission was collected from 580 to 720 nm.

Acknowledgment. This work was partially supported by a National "973" Program of China (2011CB911002), the National Natural Science Foundation of China (51002100), a Research Fund for the Doctoral Program of Higher Education of China (20103201120020), and A Project Funded by the Priority Academic Program Development of Jiangsu Higher Education Institutions.

Supporting Information Available: Photos showing GO, GO-PEG, and GO-PEG-Ce6 in various solutions; temperature curves of GO-PEG-Ce6 under laser irradiations; *in vitro* targeted delivery of Ce6 by antibody-conjugated GO-PEG. This material is available free of charge via the Internet at http://pubs.acs.org.

REFERENCES AND NOTES

1. Liu, Z.; Tabakman, S.; Chen, Z.; Dai, H. Preparation of Carbon Nanotube Bioconjugates for Biomedical Applications. *Nat. Protoc.* **2009**, *4*, 1372–1381.
2. Kostarelos, K.; Bianco, A.; Prato, M. Promises, Facts and Challenges for Carbon Nanotubes in Imaging and Therapeutics. *Nat. Nanotechnol.* **2009**, *4*, 627–633.
3. Liu, Z.; Yang, K.; Lee, S. T. Single-Walled Carbon Nanotubes in Biomedical Imaging. *J. Mater. Chem.* **2011**, *21*, 586–598.
4. Liu, Z.; Tabakman, S.; Welsher, K.; Dai, H. Carbon Nanotubes in Biology and Medicine: *in Vitro* and *in Vivo* Detection, Imaging and Drug Delivery. *Nano Res.* **2009**, *2*, 85–120.
5. Chen, Z.; Zhang, X.; Yang, R.; Zhu, Z.; Chen, Y.; Tan, W. Single-Walled Carbon Nanotubes as Optical Materials for Biosensing. *Nanoscale* **2011**, *3*, 1949–1956.
6. Zhou, X.; Huang, X.; Qi, X.; Wu, S.; Xue, C.; Boey, F. Y. C.; Yan, Q.; Chen, P.; Zhang, H. In situ Synthesis of Metal Nanoparticles on Single-Layer Graphene Oxide and Reduced Graphene Oxide Surfaces. *J. Phys. Chem. C* **2009**, *113*, 10842–10846.
7. Yin, Z.; Wu, S.; Zhou, X.; Huang, X.; Zhang, Q.; Boey, F.; Zhang, H. Electrochemical Deposition of ZnO Nanorods on Transparent Reduced Graphene Oxide Electrodes for Hybrid Solar Cells. *Small* **2010**, *6*, 307–312.
8. Li, B.; Cao, X.; Ong, H. G.; Cheah, J. W.; Zhou, X.; Yin, Z.; Li, H.; Wang, J.; Boey, F.; Huang, W. All Carbon Electronic Devices Fabricated by Directly Grown Single Walled Carbon Nanotubes on Reduced Graphene Oxide Electrodes. *Adv. Mater.* **2010**, *22*, 3058–3061.
9. Yin, Z.; Sun, S.; Salim, T.; Wu, S.; Huang, X.; He, Q.; Lam, Y. M.; Zhang, H. Organic Photovoltaic Devices Using Highly Flexible Reduced Graphene Oxide Films as Transparent Electrodes. *ACS Nano* **2010**, *4*, 5263–5268.
10. Qi, X.; Pu, K. Y.; Li, H.; Zhou, X.; Wu, S.; Fan, Q. L.; Liu, B.; Boey, F.; Huang, W.; Zhang, H. Amphiphilic Graphene Composites. *Angew. Chem., Int. Ed.* **2010**, *49*, 9426–9429.
11. Huang, X.; Li, S.; Huang, Y.; Wu, S.; Zhou, X.; Gan, C. L.; Boey, F.; Mirkin, C. A.; Zhang, H. Synthesis of Hexagonal Close-Packed Gold Nanostructures. *Nat. Commun.* **2011**, *2*, 292.
12. He, Q.; Sudibya, H.; Yin, Z.; Wu, S.; Li, H.; Boey, F.; Huang, W.; Chen, P.; Zhang, H. Centimeter-Long and Large-Scale Micropatterns of Reduced Graphene Oxide Films: Fabrication and Sensing Applications. *ACS Nano* **2010**, *4*, 3201–3208.
13. Sun, X.; Liu, Z.; Welsher, K.; Robinson, J.; Goodwin, A.; Zaric, S.; Dai, H. Nano-Graphene Oxide for Cellular Imaging and Drug Delivery. *Nano Res.* **2008**, *1*, 203–212.
14. Liu, Z.; Robinson, J.; Sun, X.; Dai, H. PEGylated Nanographene Oxide for Delivery of Water-Insoluble Cancer Drugs. *J. Am. Chem. Soc.* **2008**, *130*, 10876–10877.
15. Hu, W.; Peng, C.; Luo, W.; Lv, M.; Li, X.; Li, D.; Huang, Q.; Fan, C. Graphene-Based Antibacterial Paper. *ACS Nano* **2010**, *4*, 4317–4323.
16. Yang, K.; Zhang, S. A.; Zhang, G. X.; Sun, X. M.; Lee, S. T.; Liu, Z. A. Graphene in Mice: Ultrahigh *In Vivo* Tumor Uptake and Efficient Photothermal Therapy. *Nano Lett.* **2010**, *10*, 3318–3323.
17. Feng, L.; Liu, Z. Graphene in Biomedicine: Opportunities and Challenges. *Nanomedicine* **2011**, *6*, 317–324.
18. Li, X.; Wang, X.; Zhang, L.; Lee, S.; Dai, H. Chemically Derived, Ultrasmooth Graphene Nanoribbon Semiconductors. *Science* **2008**, *319*, 1229–1232.
19. Kim, K.; Zhao, Y.; Jang, H.; Lee, S.; Kim, J.; Ahn, J.; Kim, P.; Choi, J.; Hong, B. Large-Scale Pattern Growth of Graphene Films for Stretchable Transparent Electrodes. *Nature* **2009**, *457*, 706–710.
20. Geim, A.; Novoselov, K. The Rise of Graphene. *Nat. Mater.* **2007**, *6*, 183–191.
21. Zeng, Q.; Cheng, J.; Tang, L.; Liu, X.; Liu, Y.; Li, J.; Jiang, J. Self Assembled Graphene−Enzyme Hierarchical Nanostructures for Electrochemical Biosensing. *Adv. Funct. Mater.* **2010**, *20*, 3366–3372.
22. Zhou, M.; Zhai, Y.; Dong, S. Electrochemical Sensing and Biosensing Platform Based on Chemically Reduced Graphene Oxide. *Anal. Chem.* **2009**, *81*, 5603–5613.
23. Mohanty, N.; Berry, V. Graphene-Based Single-Bacterium Resolution Biodevice and DNA Transistor: Interfacing Graphene Derivatives with Nanoscale and Microscale Biocomponents. *Nano Lett.* **2008**, *8*, 4469–4476.
24. Tang, L. A. L.; Wang, J.; Loh, K. P. Graphene-Based SELDI Probe with Ultrahigh Extraction and Sensitivity for DNA Oligomer. *J. Am. Chem. Soc.* **2010**, *132*, 10976–10977.
25. Balapanuru, J.; Yang, J. X.; Xiao, S.; Bao, Q.; Jahan, M.; Polavarapu, L.; Wei, J.; Xu, Q. H.; Loh, K. P. A Graphene Oxide−Organic Dye Ionic Complex with DNA Sensing and Optical Limiting Properties. *Angew. Chem., Int. Ed.* **2010**, *49*, 6549–6553.
26. He, S.; Song, B.; Li, D.; Zhu, C.; Qi, W.; Wen, Y.; Wang, L.; Song, S.; Fang, H.; Fan, C. A Graphene Nanoprobe for Rapid, Sensitive, and Multicolor Fluorescent DNA Analysis. *Adv. Funct. Mater.* **2010**, *20*, 453–459.
27. Wen, Y.; Xing, F.; He, S.; Song, S.; Wang, L.; Long, Y.; Fan, C. A Graphene-Based Fluorescent Nanoprobe for Silver (I) Ions Detection by Using Graphene Oxide and a Silver-Specific Oligonucleotide. *Chem. Commun.* **2010**, *46*, 2596–2598.
28. Loh, K. P.; Bao, Q.; Eda, G.; Chhowalla, M. Graphene Oxide as a Chemically Tunable Platform for Optical Applications. *Nat. Chem.* **2010**, *2*, 1015–1024.
29. Cao, X.; He, Q.; Shi, W.; Li, B.; Zeng, Z.; Shi, Y.; Yan, Q.; Zhang, H. Graphene Oxide as a Carbon Source for Controlled Growth of Carbon Nanowires. *Small* **2011**, *7*, 1199–1202.
30. Wang, Z.; Zhang, J.; Chen, P.; Zhou, X.; Yang, Y.; Wu, S.; Niu, L.; Han, Y.; Wang, L.; Boey, F. Label-free, Electrochemical Detection of Methicillin-Resistant Staphylococcus Aureus DNA with Reduced Graphene Oxide-Modified Electrodes. *Biosens. Bioelectron.* **2011**, *26*, 3881–3886.
31. Zhang, L.; Xia, J.; Zhao, Q.; Liu, L.; Zhang, Z. Functional Graphene Oxide as a Nanocarrier for Controlled Loading and Targeted Delivery of Mixed Anticancer Drugs. *Small* **2010**, *6*, 537–544.
32. Yang, X.; Wang, Y.; Huang, X.; Ma, Y.; Huang, Y.; Yang, R.; Duan, H.; Chen, Y. Multi-Functionalized Graphene Oxide based Anticancer Drug-Carrier with Dual-Targeting Function and pH-Sensitivity. *J. Mater. Chem.* **2010**, *21*, 3449–3454.
33. Huang, P.; Xu, C.; Lin, J.; Wang, C.; Wang, X.; Zhang, C.; Zhou, X.; Guo, S.; Cui, D. Folic Acid-Conjugated Graphene Oxide Loaded with Photosensitizers for Targeting Photodynamic Therapy. *Theranostics* **2011**, *1*, 240–250.
34. Dong, H. Q.; Zhao, Z. L.; Wen, H. Y.; Li, Y. Y.; Guo, F. F.; Shen, A. J.; Pilger, F.; Lin, C.; Shi, D. L. Poly (Ethylene Glycol) Conjugated Nano-Graphene Oxide for Photodynamic Therapy. *Sci. China Ser. B* **2010**, *53*, 2265–2271.
35. Feng, L.; Zhang, S.; Liu, Z. Graphene Based Gene Transfection. *Nanoscale* **2011**, *3*, 1252–1257.

36. Zhang, L.; Lu, Z.; Zhao, Q.; Huang, J.; Shen, H.; Zhang, Z. Enhanced Chemotherapy Efficacy by Sequential Delivery of siRNA and Anticancer Drugs Using PEI Grafted Graphene Oxide. *Small* **2011**, *7*, 460–467.
37. Yang, K.; Wan, J.; Zhang, S.; Zhang, Y.; Lee, S. T.; Liu, Z. *In Vivo* Pharmacokinetics, Long-Term Biodistribution, and Toxicology of PEGylated Graphene in Mice. *ACS Nano* **2011**, *5*, 516–522.
38. Dolmans, D. E.; Dai Fukumura, R. K. J. Photodynamic Therapy for Cancer. *Nat. Rev. Cancer* **2003**, *3*, 380–387.
39. Hasan, T.; Parrish, J. Photodynamic Therapy of Cancer. *Cancer Med.* **1996**, *50*, 739–751.
40. Henderson, B.; Dougherty, T. How Does Photodynamic Therapy Work? *Photochem Photobiol.* **1992**, *55*, 145–157.
41. Konan, Y.; Gurny, R.; Allémann, E. State of the Art in the Delivery of Photosensitizers for Photodynamic Therapy. *J. Photochem. Photobiol. B* **2002**, *66*, 89–106.
42. Austin, T.; Truant, G. Hyperthermia, Antipyretics and Function of Polymorphonuclear Leukocytes. *Can. Med. Assoc. J.* **1978**, *118*, 493–495.
43. Fraker, D. L.; Alexander, H. R.; Andrich, M.; Rosenberg, S. A. Treatment of Patients with Melanoma of the Extremity using Hyperthermic Isolated Limb Perfusion with Melphalan, Tumor Necrosis Factor, and Interferon Gamma: Results of a Tumor Necrosis Factor Dose-Escalation Study. *J. Clin. Oncol.* **1996**, *14*, 479–489.
44. Wust, P.; Hildebrandt, B.; Sreenivasa, G.; Rau, B.; Gellermann, J.; Riess, H.; Felix, R.; Schlag, P. Hyperthermia in Combined Treatment of Cancer. *Lancet Oncol.* **2002**, *3*, 487–497.
45. Storm, F. K.; Harrison, W. H.; Elliott, R. S.; Morton, D. L. Normal Tissue and Solid Tumor Effects of Hyperthermia in Animal Models and Clinical Trials. *Cancer Res.* **1979**, *39*, 2245–2251.
46. Markovic, Z. M.; Harhaji-Trajkovic, L. M.; Todorovic-Markovic, B. M.; Kepic, D. P.; Arsikin, K. M.; Jovanovic, S. P.; Pantovic, A. C.; Dramicanin, M. D.; Trajkovic, V. S. *In Vitro* Comparison of the Photothermal Anticancer Activity of Graphene Nanoparticles and Carbon Nanotubes. *Biomaterials* **2011**, *32*, 1121–1129.
47. Moon, H. K.; Lee, S. H.; Choi, H. C. *In Vivo* Near-Infrared Mediated Tumor Destruction by Photothermal Effect of Carbon Nanotubes. *ACS Nano* **2009**, *3*, 3707–3713.
48. Robinson, J. T.; Welsher, K.; Tabakman, S. M.; Sherlock, S. P.; Wang, H.; Luong, R.; Dai, H. High Performance *in Vivo* Near-IR (> 1 m) Imaging and Photothermal Cancer Therapy with Carbon Nanotubes. *Nano Res.* **2010**, *3*, 779–793.
49. Liu, X.; Tao, H.; Yang, K.; Zhang, S.; Lee, S. T.; Liu, Z. Optimization of Surface Chemistry on Single-Walled Carbon Nanotubes for *in Vivo* Photothermal Ablation of Tumors. *Biomaterials* **2011**, *32*, 144–151.
50. von Maltzahn, G.; Park, J. H.; Agrawal, A.; Bandaru, N. K.; Das, S. K.; Sailor, M. J.; Bhatia, S. N. Computationally Guided Photothermal Tumor Therapy Using Long-Circulating Gold Nanorod Antennas. *Cancer Res.* **2009**, *69*, 3892–3900.
51. Choi, W. I.; Kim, J. Y.; Kang, C.; Byeon, C. C.; Kim, Y. H.; Tae, G. Tumor Regression *in Vivo* by Photothermal Therapy Based on Gold-Nanorod-Loaded, Functional Nanocarriers. *ACS Nano* **2011**, *5*, 1995–2003.
52. Sherlock, S. P.; Tabakman, S. M.; Xie, L.; Dai, H. Photothermally Enhanced Drug Delivery by Ultrasmall Multifunctional FeCo/Graphitic Shell Nanocrystals. *ACS Nano* **2011**, *5*, 1505–1512.
53. Liu, Z.; Fan, A.; Rakhra, K.; Sherlock, S.; Goodwin, A.; Chen, X.; Yang, Q.; Felsher, D.; Dai, H. Supramolecular Stacking of Doxorubicin on Carbon Nanotubes for *in Vivo* Cancer Therapy. *Angew. Chem., Int. Ed.* **2009**, *48*, 7668–7672.
54. Liu, Z.; Sun, X.; Nakayama-Ratchford, N.; Dai, H. Supramolecular Chemistry on Water-Soluble Carbon Nanotubes for Drug Loading and Delivery. *ACS Nano* **2007**, *1*, 50–56.
55. Kralji, I.; Mohsni, S. A New Method for the Detection of Singlet Oxygen in Aqueous Solutions. *Photochem. Photobiol.* **1978**, *28*, 577–581.
56. Zhu, Z.; Tang, Z.; Phillips, J. A.; Yang, R.; Wang, H.; Tan, W. Regulation of Singlet Oxygen Generation using Single-Walled Carbon Nanotubes. *J. Am. Chem. Soc.* **2008**, *130*, 10856–10857.
57. Levi-Polyachenko, N. H.; Merkel, E. J.; Jones, B. T.; Carroll, D. L.; Stewart, J. H., IV. Rapid Photothermal Intracellular Drug Delivery using Multiwalled Carbon Nanotubes. *Mol. Pharmaceut.* **2009**, *6*, 1092–1099.
58. Ogura, S.; Fujita, Y.; Kamachi, T.; Okura, I. Preparation of Chlorin e6−Monoclonal Antibody Conjugate and its Effect For Photodynamic Therapy. *J. Porphyrins Phthalocyanines* **2001**, *5*, 486–489.